Title

Structural constitutive modeling of the anisotropic mechanical properties of human vocal fold lamina propria

Journal

The Journal of the Acoustical Society of America, 145(6)

ISSN

0001-4966

Author

Zhang, Zhaoyan

Publication Date

2019-06-01

DOI

10.1121/1.5109794

Peer reviewed

Structural constitutive modeling of the anisotropic mechanical properties of human vocal fold lamina propria

Zhaoyan Zhang
Department of Head and Neck Surgery, University of California, Los Angeles, 31-24 Rehab Center, 1000 Veteran Avenue, Los Angeles, California 90095-1794, USA
zyzhang@ucla.edu

Abstract: The anisotropic mechanical properties of the vocal fold lamina propria play an important role in voice production and control. The goal of this study is to develop a constitutive model capable of predicting lamina propria elastic moduli along both the longitudinal and transverse directions under different conditions of vocal fold elongation, which can be used as input to reduced-order phonation models based on linear elasticity. A structurally-based constitutive model that links microstructural characteristics of the lamina propria to its macromechanical properties is proposed. The model prediction has been shown to agree reasonably well with recent biaxial tensile testing results.

[AL]
Date Received: March 19, 2019 **Date Accepted:** May 7, 2019

1. Introduction

The lamina propria of the human vocal folds is known to exhibit a nonlinear, anisotropic mechanical behavior, due to the presence of collagen and elastin fibers aligned primarily along the anterior-posterior (AP) direction. This nonlinear, anisotropic mechanical behavior, together with laryngeal muscle activation, plays an important role in human voice production and control. For example, regulation of the longitudinal stiffness and tension through vocal fold elongation is considered the primary mechanism of pitch control (Zhang, 2016a), whereas the stiffness in the transverse or coronal plane has an important role in determining the vocal fold vibration pattern and voice quality (Hirano and Kakita, 1985; Story and Titze, 1995; Zhang, 2018). An important goal of voice production research is to develop a constitutive model that describes this nonlinear, anisotropic mechanical behavior.

While such constitutive models can be phenomenologically-based (e.g., Alipour-Haghighi and Titze, 1991), adopting a mathematical function that best describes experimentally-measured stress-strain data (e.g., the widely-used Fung-type model), a structurally-based constitutive model that relates the macromechanical behavior to the underlying microstructural features of the constituent components such as collagen, elastin, and the non-fibrous ground matrix (Kelleher *et al.*, 2013; Miri *et al.*, 2013) is more appealing. Such a structurally-based constitutive model would provide a clearer structure-function relationship, thus allowing direct prediction of changes in the mechanical behavior of the lamina propria due to microstructural tissue changes resulting from aging or vocal pathology, and analysis of the mechanical behavior of tissue engineered vocal fold replacement. This approach would also allow evaluation of the mechanical properties of the individual layers of the lamina propria, which otherwise are difficult to measure experimentally.

This study presents our first step toward developing such a structurally-based constitutive model of the lamina propria. In comparison to previous studies that compared their models to stress-strain data from uniaxial testing and indentation tests (Kelleher *et al.*, 2013; Miri *et al.*, 2013), we focus on developing a model that is able to predict the anisotropic stress-strain data from biaxial tensile testing of human lamina propria. Compared with uniaxial tensile tests or indentation tests, biaxial tensile testing allows a better quantification of the anisotropic mechanical properties at different vocal fold longitudinal elongations and vibration amplitudes in the transverse plane, thus better approximating the realistic mechanical conditions that occur in human phonation. Indeed, the results from our recent biaxial tensile testing (Zhang *et al.*, 2017) showed a strong mechanical coupling between the AP and transverse directions that was not observed in uniaxial tensile tests.

Toward application to computational simulation of phonation, the model is then used to calculate the AP and transverse elastic moduli at different vocal fold

elongations for two microstructural states that approximate those of the superficial and deep layers of the human lamina propria. This capability of the model to provide physically-consistent tangent elastic moduli along both the AP and transverse directions is particularly important for reduced-order models based on linear elasticity (e.g., Titze and Talkin, 1979; Zhang, 2016b), which are computationally efficient and thus have the potential toward practical applications. Currently these elastic moduli are specified empirically in computational simulations, often neglecting their covariation during voice production.

2. Model

One of the first comprehensive structurally-based constitutive models was proposed by Lanir (1983) for fibrous connective tissues. The idea is that the mechanical behavior of soft tissues results from the deformations and interactions between the constituent components, which in the vocal folds include collagen, elastin, and non-fibrous ground matrix. In particular, tissue nonlinearity results from the gradual straightening or recruitment of the wavy collagen and elastin fibers. In voice literature, the idea that collagen recruitment contributes to vocal fold material nonlinearity has been described as early as in van den Berg and Tan (1959), and was experimentally verified in our recent study (Fata *et al.*, 2013), the findings of which are summarized below. Combining uniaxial tensile testing with multiphoton microscopy, we simultaneously measured the macro-structural stress-strain curve and the recruitment pattern of collagen and elastin fibers when the human lamina propria was subject to longitudinal tension (Fig. 1). Microscopic imaging showed that the collagen and elastin fibers were wavy at the unloaded resting state [Fig. 1(b)]. The fibers were oriented mostly along the AP direction, with a standard deviation of about 9° to 16.5° in the fiber orientation angle. With increasing longitudinal tension, the fibers gradually became straightened, thus load-bearing [Fig. 1(c)]. The percentage of fibers that were recruited to bear load was calculated as the percentage of fibers straightened weighted by individual collagen thickness. The main finding was that the recruitment curve of collagen fibers followed closely to the stress-strain curve [Fig. 1(a)], indicating a dominant contribution of collagen recruitment to the overall longitudinal tissue mechanical behavior, whereas elastin recruitment was responsible for the small nonlinearity in the small-moderate strain range.

Based on the above findings, a structural constitutive model is developed similar to Lanir (1983) and Fan and Sacks (2014). The strain energy function W includes contributions from the non-fibrous ground matrix W_m, the recruitment of the collagen fibers W_c and elastin fibers W_e, and potential fiber-matrix interaction W_{fmi}, respectively, weighted by their respective volume fractions

$$W = \phi_m W_m + \phi_c W_c + \phi_e W_e + W_{fmi} + p(J-1), \tag{1}$$

where ϕ_m, ϕ_c, ϕ_e are the volume fractions of the matrix, collagen, and elastin fibers, respectively, J is the determinant of the vocal fold deformation gradient, and p is the Lagrange multiplier. The last term in Eq. (1) is included to enforce tissue incompressibility, and the Lagrange multiplier p is determined by the boundary condition

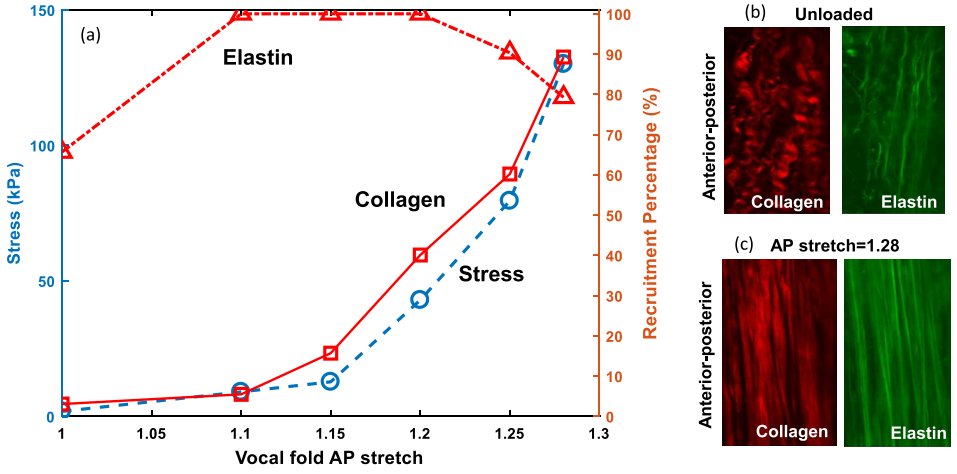

Fig. 1. (Color online) (a) The recruitment function of the collagen fibers (solid line) follows closely to the simultaneously measured stress-strain curve (dashed line) of a human vocal fold lamina propria subject to uniaxial tensile testing, while elastin recruitment (dashed-dotted line) is responsible for small nonlinearity in the small to moderate strain range. (b) Collagen and elastin fibers are wavy at the resting unloaded state, and (c) become gradually straightened with increasing longitudinal tension. Data from Fata *et al.* (2013).

(e.g., zero out-of-plane stress in a biaxial tensile test). The non-fibrous matrix is modeled as an isotropic Neo-Hookean material $W_m = (\mu/2)(I_1 - 3)$, where μ is the shear modulus and I_1 is the first invariant of the deformation tensor.

Considering the fibers are primarily aligned along the AP direction within the lamina propria, we assume a planar distribution of fibers, and approximate the fiber orientation by a Gaussian distribution $\rho(\theta)$, with a preferred direction $\theta = 0$ along the AP direction and a standard deviation of σ quantifying the dispersion of fiber orientation. As in Lanir (1983), each single fiber is assumed to have a linear stress-strain relation modeled by a strain energy function $(K/2)\varepsilon^2$, where K is the elastic modulus of the individual straight fibers and $\varepsilon = N^T E N$ is the fiber strain along the fiber direction N when subject to a Green strain tensor E. Because the fibers are crimped at the resting state, the fibers would need to be straightened first before they begin to experience strain. Assuming the strain required to straighten an individual fiber is ε_s, the true fiber strain is then related to the fiber strain by $\varepsilon_t = (\varepsilon - \varepsilon_s)/(1 + 2\,\varepsilon_s)$. Similar to Fan and Sacks (2014), we assume that the portion of fibers with a specific straightening strain ε_s follows a Beta distribution,

$$D(\varepsilon_s) = \begin{cases} \dfrac{x^{\alpha-1}(1-x)^{\beta-1}}{B(\alpha,\beta)(\varepsilon_{ub} - \varepsilon_{lb})}, & x = \dfrac{\varepsilon_s - \varepsilon_{lb}}{\varepsilon_{ub} - \varepsilon_{lb}} \in [0,1] \\ 0, & \text{otherwise}, \end{cases} \tag{2}$$

where ε_{lb} and ε_{ub} are the lower and upper bounds of ε_s, and B(α, β) is the Beta function with shape parameters (α, β). The strain energy functions associated with the recruitment of the collagen and elastin fibers are then expressed as the summation over different fiber orientations,

$$W_c = \frac{K_c}{2}\int_{-\pi/2}^{\pi/2} \rho_c(\theta) \int_0^{\varepsilon} D_c(\varepsilon_{s,c}) \left(\frac{\varepsilon - \varepsilon_{s,c}}{1 + 2\varepsilon_{s,c}}\right)^2 d\varepsilon_{s,c} d\theta, \tag{3}$$

$$W_e = \frac{K_e}{2}\int_{-\pi/2}^{\pi/2} \rho_e(\theta) \int_0^{\varepsilon} D_e(\varepsilon_{s,e}) \left(\frac{\varepsilon - \varepsilon_{s,e}}{1 + 2\varepsilon_{s,e}}\right)^2 d\varepsilon_{s,e} d\theta, \tag{4}$$

where the subscripts c and e denote collagen and elastin fibers, respectively.

The inclusion of the fiber-matrix interaction term is based on the observation in biaxial tensile testing (Zhang *et al.*, 2017) that AP elongation significantly increases the transverse stiffness. Our initial modeling effort showed that this cross-axis coupling is stronger than that would be predicted by fiber dispersion alone and thus an explicit fiber-matrix interaction term is required for the model to successfully curve fit the biaxial testing data. Since such coupling is stronger at strain ranges with collagen recruitment (Zhang *et al.*, 2017), only collagen-matrix interaction is considered in Eq. (1) for simplicity,

$$W_{fmi} = \phi_m \mu \phi_c K_c \frac{1}{2}\int_{-\pi/2}^{\pi/2} \rho_c(\theta) \int_0^{\varepsilon} D_c(\varepsilon_{s,c})(I_1 - 3) \left(\frac{\varepsilon - \varepsilon_{s,c}}{1 + 2\varepsilon_{s,c}}\right)^2 d\varepsilon_{s,c} d\theta. \tag{5}$$

The total second Piola–Kirchhoff stress S is

$$\begin{aligned} S &= S_m + S_c + S_e + S_{fmi} + pC^{-1}, \\ S_m &= \phi_m \mu I, \\ S_c &= \phi_c K_c \int_{-\pi/2}^{\pi/2} \rho_c(\theta) \int_0^{\varepsilon} D_c(\varepsilon_s) \frac{\varepsilon - \varepsilon_s}{(1 + 2\varepsilon_s)^2} (N \otimes N) d\varepsilon_s d\theta, \\ S_e &= \phi_e K_e \int_{-\pi/2}^{\pi/2} \rho_e(\theta) \int_0^{\varepsilon} D_e(\varepsilon_s) \frac{\varepsilon - \varepsilon_s}{(1 + 2\varepsilon_s)^2} (N \otimes N) d\varepsilon_s d\theta, \\ S_{fmi} &= \phi_m \mu \phi_c K_c \int_{-\pi/2}^{\pi/2} \rho_c(\theta) \int_0^{\varepsilon} D_c(\varepsilon_s)(I_1 - 3) \frac{\varepsilon - \varepsilon_s}{(1 + 2\varepsilon_s)^2} (N \otimes N) d\varepsilon_s d\theta \\ &\quad + \phi_m \mu \phi_c K_c \int_{-\pi/2}^{\pi/2} \rho_c(\theta) \int_0^{\varepsilon} D_c(\varepsilon_s) \left(\frac{\varepsilon - \varepsilon_s}{1 + 2\varepsilon_s}\right)^2 I d\varepsilon_s d\theta, \end{aligned} \tag{6}$$

where C is the Green deformation tensor and I is the identify tensor.

In summary, the control parameters of the model include $(\sigma, \alpha, \beta, \varepsilon_{lb}, \varepsilon_{ub})_c$ and $(\sigma, \alpha, \beta, \varepsilon_{lb}, \varepsilon_{ub})_e$ for collagen and elastin fiber orientation dispersion and recruitment, and $(\phi_m\mu, \phi_c K_c, \phi_e K_e)$ for elastic moduli of different constituent components.

3. Comparison to experiments

Biaxial tensile testing was performed to investigate the model's capability to explain experimental data. The lamina propria layer of a male larynx was dissected and used in the tensile tests. The same experimental setup and procedure as described in Zhang *et al.* (2017) was used, with a five-test protocol. In the first test, the specimen was vibrated sinusoidally along the AP direction while the transverse direction was held constant at zero strain. In the other four tests, the specimen was vibrated along the transverse direction while being held anterior-posteriorly at four different constant AP strains. Figure 2 shows the measured stresses along both the AP (left figure) and transverse directions (right figure) as a function of the stretch along the direction of imposed sinusoidal vibration (AP stretch for the first test and transverse strain for the other four tests).

The model is then curve fitted to the biaxial testing data to estimate the model parameters, using the "lsqcurvefit" function in MATLAB. To differentiate the contributions of collagen and elastin fibers, the upper bound of the parameter ε_{ub} for elastin is set to 0.15, which enforces the elastin fibers to be fully recruited at small strains, whereas the upper bound of ε_{ub} for collagen is set to 1.0, allowing gradual collagen recruitment. The estimated model parameters are listed in Table 1 (first row), and the corresponding model prediction is shown in Fig. 2, which shows a good agreement with the experimental data. It should be noted that, unlike uniaxial tensile testing which measures stress and strain along only one direction and thus generally can be curve fitted to a reasonable agreement, biaxial tensile testing measures stresses along two directions simultaneously and thus has a more stringent requirement on the model in order to reach a good performance of curve fitting. For example, the agreement is notably lower without the fiber-matrix interaction term. This is because without this interaction term, the large increase in the transverse stress with increasing AP strain would require a large degree of fiber dispersion, which then would under predict the simultaneous increase in the AP stress.

The estimated model parameters are generally comparable to those available in the literature. The estimated shear modulus of the ground matrix is in the same order of magnitude of those reported in previous studies (Chan and Rodriguez, 2008; Kelleher *et al.*, 2013) and used in computational models (e.g., Titze and Talkin, 1979; Zhang, 2018). The elastic moduli of the collagen and elastin fibers are generally comparable to, but slightly smaller than, those reported in Miri *et al.* (2013). The estimated standard deviation of collagen fiber orientation (16.3°) is similar to that measured (9°–16.5°) in Fata *et al.* (2013). This general agreement, together with the model's ability to match stress data along both directions for the five biaxial tests in Fig. 2, indicates that the proposed model is a reasonable representation of the underlying structural mechanics of lamina propria.

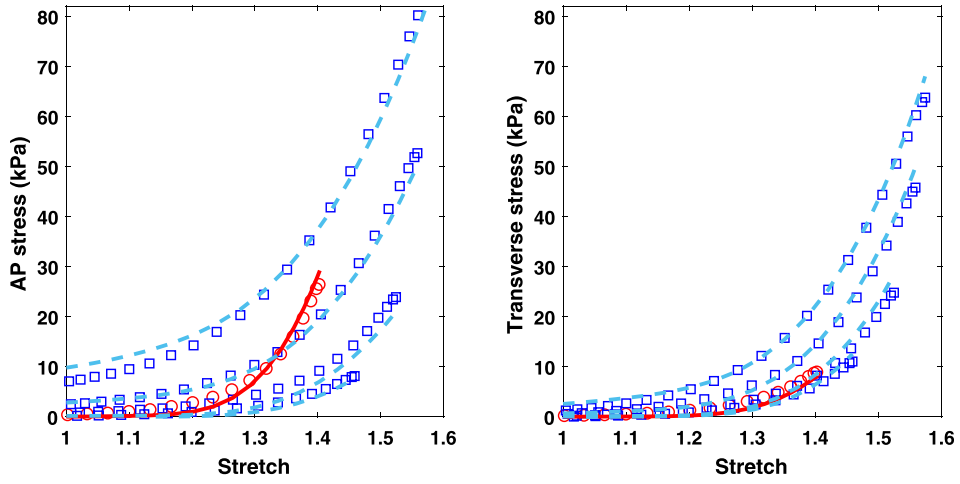

Fig. 2. (Color online) Comparison between model prediction (solid and dashed lines) and experimental measurement (symbols) of the AP (left) and transverse (right) stresses of a human vocal fold lamina propria subject to biaxial tensile testing. Circle symbols: the specimen was sinusoidally vibrated along the AP direction while being held at a constant strain along the transverse direction. Square symbols: the specimen was sinusoidally vibrated along the transverse direction while being held at different constant strains along the AP direction.

Table 1. Model parameters estimated from curve fitting the biaxial tensile testing data (first row) and adapted for a hypothetical superficial lamina propria layer with reduced collagen and elastin volume fractions and increased fiber dispersion (second row).

	Matrix	Collagen			Elastin		
	$\phi_m\mu$(kPa)	$\phi_c K_c$(kPa)	σ (°)	α, β, ε_{lb}, ε_{ub}	$\phi_e K_e$(kPa)	σ (°)	α, β, ε_{lb}, ε_{ub}
1	1.0	202.0	16.3	(5.4, 5.4, 0, 0.53)	5	18.3	(1.07, 9.87, 0, 0.05)
2	1.0	20.2	36	(5.4, 5.4, 0, 0.53)	0.5	36	(1.07, 9.87, 0, 0.05)

4. Anisotropic elastic moduli of vocal fold cover and ligament

A motivation of the present study is to develop a constitutive model that is able to predict the anisotropic elastic moduli of the lamina propria at different vocal fold elongations. As an example, two structural composition conditions of the lamina propria are considered. The first condition has the same model parameters as estimated from the curve fitting described above (first row, Table 1). Since the curve fitting is performed to match biaxial tensile testing data from an entire lamina propria layer, it can be assumed that this condition may represent that of the intermediate and deep layers of the lamina propria (i.e., vocal ligament), which are known to have a dense distribution of collagen and elastin fibers. The second condition (second row, Table 1) is designed to approximate the superficial layer of the lamina propria, which has been shown to have limited and loose elastin and collagen fibers with increased fiber dispersion (Hirano and Kakita, 1985). This condition is modified from the first condition to represent these differences, by reducing volume fractions of the collagen and elastin fibers by a factor of ten and increasing fiber dispersion to 36°.

For each structural condition, biaxial tensile testing is simulated at different conditions of vocal fold AP elongation ε_{ap} and transverse deformation ε_t, from which tangent moduli are calculated. For example, to calculate the AP stiffness at the condition ($\varepsilon_{ap}=0.2$, $\varepsilon_t=0.1$), a biaxial tensile test is simulated by elongating the lamina propria by 20% and then imposing a sinusoidal motion along the AP direction while simultaneously imposing a constant strain of 0.1 along the transverse direction. The AP stiffness is then calculated by a linear curve fitting between the AP stress and AP strain. The transverse stiffness is calculated similarly, except that the sinusoidal vibration is imposed along the transverse direction. The results are shown in Fig. 3 for both structural conditions. Similar to Zhang *et al.* (2017), Fig. 3 shows that AP elongation not only increases the AP stiffness, but also significantly increases the transverse stiffness, particularly when elongation leads to recruitment of collagen fibers (for stretches above 1.1). Similarly, increased transverse deformation (e.g., as occurs with increasing vocal fold vibration amplitude) can also increase both the transverse and AP stiffnesses. Compared with the first condition (left panel in Fig. 3), the second condition (right panel in Fig. 3), which simulates the superficial layer of the lamina propria, exhibits much reduced nonlinearity and a smaller degree of stiffness anisotropy between the AP and transverse directions, resulting in an overall softer mechanical response.

5. Discussion and conclusion

In this study we show that the proposed structurally-based constitutive model is able to match biaxial tensile testing data, and the estimated model parameters are generally in the range reported in the literature. Compared with phenomenologically-based constitutive models, this model would allow us to predict the anisotropic stiffness conditions of the lamina propria, given microstructural composition information of the specific layer of the lamina propria, as demonstrated above. Such anisotropic stiffness information can then be used to develop phonation models that better represent the layer-wise distinction in mechanical properties of the lamina propria, or subject-specific phonation models with a mechanical behavior that varies with age or pathology.

This study can be improved in many aspects. First, while the proposed model is able to curve fit biaxial tensile testing data and the estimated model parameters are in general consistent with observations from microscopic imaging, direct validation of the model would require simultaneously acquiring biaxial stress-strain data and microstructural changes of the collagen and elastin fibers in the same specimen. Such experimental studies would also provide insight into how the stiffness of collagen and elastin fibers varies across subjects, age, or vocal pathologies, facilitating the development of subject-specific models. Also, due to the mechanical coupling between the AP and

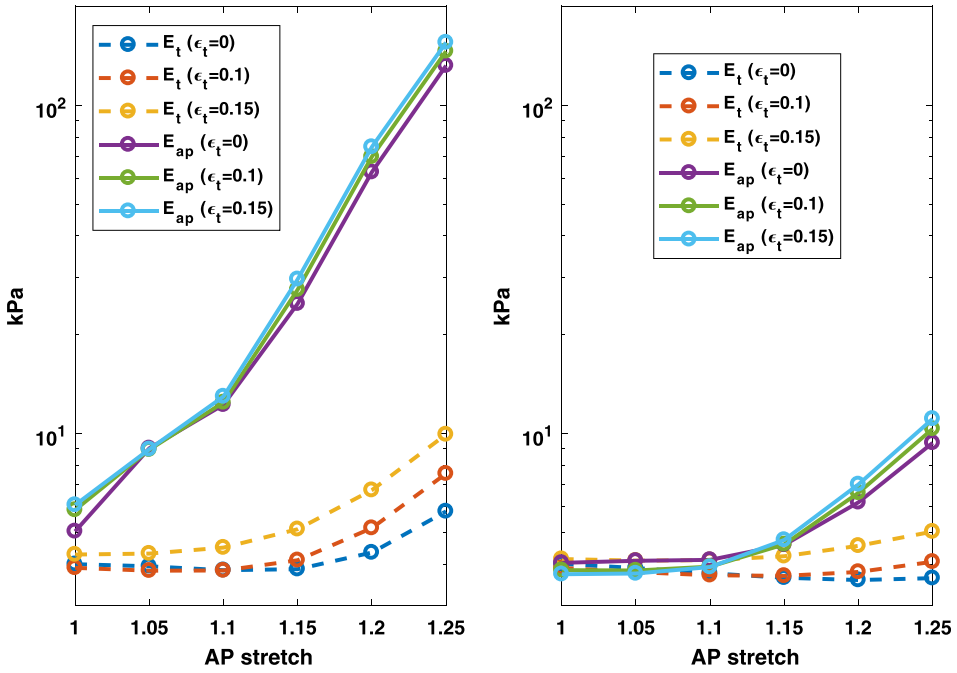

Fig. 3. (Color online) Tangent elastic moduli along the AP (E_{ap}) and transverse directions (E_t) as a function of AP stretch for different transverse deformations (ε_t). These moduli are predicted by the proposed model using the model parameters listed in the first (left) and second (right) row of Table 1, which simulate the intermediate/deep layer and the superficial layer of the lamina propria, respectively.

transverse directions observed in the biaxial testing data, the proposed model includes a fiber-matrix interaction term. While the current formulation of this interaction term allows a reasonably good curve fitting of the biaxial testing data, it is desirable to develop a formulation that reflects the physiological mechanisms of fiber-matrix interaction and that is based on experimentally measurable microstructural properties. These issues will be addressed in future studies.

Acknowledgments

This study was supported by research Grant Nos. R01 DC009229 and R01DC011299 from the National Institute on Deafness and Other Communication Disorders, the National Institutes of Health.

References and links

Alipour-Haghighi, F., and Titze, I. R. (**1991**). "Elastic models of vocal fold tissues," J. Acoust. Soc. Am. **90**, 1326–1331.

Chan, R. W., and Rodriguez, M. (**2008**). "A simple-shear rheometer for linear viscoelastic characterization of vocal fold tissues at phonatory frequencies," J. Acoust. Soc. Am. **124**(2), 1207–1219.

Fan, R., and Sacks, M. S. (**2014**). "Simulation of planar soft tissues using a structural constitutive model: Finite element implementation and validation," J. Biomech. **47**, 2043–2054.

Fata, B., Vergara, J., and Zhang, Z. (**2013**). "Direct characterization of collagen recruitment in the human vocal fold lamina propria," J. Acoust. Soc. Am. **134**, 4204.

Hirano, M., and Kakita, Y. (**1985**). "Cover-body theory of vocal fold vibration," in *Speech Science: Recent Advances*, edited by R. G. Daniloff (College-Hill Press, San Diego, CA), pp. 1–46.

Lanir, Y. (**1983**). "Constitutive equations for fibrous connective tissues," J. Biomech. **16**(1), 1–12 (1983).

Kelleher, J. E., Siegmund, T., Du, M., Naseri, E., and Chan, R. W. (**2013**). "The anisotropic hyperelastic biomechanical response of the vocal ligament and implications for frequency regulation: A case study," J. Acoust. Soc. Am. **133**, 1625–1636.

Miri, A. K., Heris, H. K., Tripathy, U., Wiseman, P. W., and Mongeau, L. (**2013**). "Microstructural characterization of vocal folds toward a strain energy model of collagen remodeling," Acta Biomater. **9**, 7957–7967.

Story, B. H., and Titze, I. R. (**1995**). "Voice simulation with a body-cover model of the vocal folds," J. Acoust. Soc. Am. **97**, 1249–1260.

Titze, I., and Talkin, D. (**1979**). "A theoretical study of the effects of various laryngeal configurations on the acoustics of phonation," J. Acoust. Soc. Am. **66**, 60–74.

van den Berg, J. W., and Tan, T. S. (**1959**). "Results of experiments with human larynxes," Pract. Otorhinolaryngol. **21**, 425–450.

Zhang, Z. (**2016a**). "Mechanics of human voice production and control," J. Acoust. Soc. Am. **140**(4), 2614–2635.

Zhang, Z. (**2016b**). "Cause-effect relationship between vocal fold physiology and voice production in a three-dimensional phonation model," J. Acoust. Soc. Am. **139**, 1493–1507.

Zhang, Z. (**2018**). "Vocal instabilities in a three-dimensional body-cover phonation model," J. Acoust. Soc. Am. **144**(3), 1216–1230.

Zhang, Z., Samajder, H., and Long, J. (**2017**). "Biaxial mechanical properties of human vocal fold cover under vocal fold elongation," J. Acoust. Soc. Am. **142**, EL356–EL361.